Ref. Ares(2026)942916 - 27/01/2026

SOMMER

Solar-Based Membrane Reactor for Syngas Production

D2.7 – Report on mechanical stability of slip-casted and 3D-printed membranes samples at high temperature

WP2 – Development & Manufacturing of Membrane Components

31/01/2026

Funded by the European Union

Disclaimer

Acknowledgement

The project SOMMER is funded by the European Union under Grant Agreement Number 101118293.

Document Identifier

Grant Agreement No.	**101118293**		**Acronym**	**SOMMER**
Title	Solar-based membrane reactor for syngas production			
Call Topic	HORIZON-CL5-2022-D3-02-06			
Type of action	HORIZON EUROPE, RIA - Research and Innovation Actions			
Start date	01.11.2023		**Duration**	48 months
Project URL	https://sommer-project.eu/			
Project Officer	Dr. Luca Bondi			
Project Coordinator	DLR - German Aerospace Center			
Deliverable	D2.7 - Report on mechanical stability of slip-casted and 3D-printed membranes samples at high temperature			
Date of Delivery	**Contractual**	31.01.2026	**Actual**	27.01.2026
Nature	Report	**Dissemination level**		PU
Lead Beneficiary	FZJ			
Responsible Author	Stefan Baumann, s.baumann@fz-juelich.de			
Contributors	Kevin Streckel (FZJ), k.streckel@fz-juelich.de Jürgen Malzbender (FZJ) j.malzbender@fz-juelich.de			
Reviewers	Nicolas Kruse (DLR), nicolas.kruse@dlr.de Asmaa Eltayeb (DLR), asmaa.eltayeb@dlr.de			

Funded by the European Union

About the Project

SOMMER aims to develop and demonstrate an innovative carbon-neutral process for syngas production by directly integrating solar energy into a catalytic membrane reactor, facilitating the decomposition of H_2O and CO_2 (e.g., captured from carbon-emitting industries or through direct air capture). This approach enables SOMMER to overcome reliance on fossil-based energy for syngas production, utilizing CO_2 instead of natural gas as a feedstock. Syngas, a critical intermediate for the chemical industry, prompts SOMMER to encompass the entire value chain - from CO_2 provision in a cement plant to syngas formation and further processing into valuable products like DME or methanol. The core of SOMMER's technology is the optimized energy integration of a novel thermochemical conversion process of CO_2 and H_2O in a single step. This process is supported by highly selective catalysts, a dual-phase composite membrane, and a concentrated solar-thermal plant fulfilling the thermal energy demand. The key outcomes of SOMMER involve the experimental demonstration and evaluation of the innovative solar-powered membrane technology. Additionally, it focuses on developing high-performance, cost-effective membranes as pivotal components, elevating the technology to new heights. SOMMER's strategy involves advancing membrane manufacturing through slip-casting, a more mature approach, and additive manufacturing to optimize the effective membrane surface area in the reactor. The concept anticipates future advantages, allowing prolonged and flexible operation by seamlessly switching between two operational cases: I) purely solar approach at 1500 °C and II) a biogas-supported approach at 900 °C. Furthermore, SOMMER aims to identify the technological, ecological, and economical potential for flexible and highly efficient solar syngas production, contributing to the formulation of a detailed roadmap and providing a foundation for pre-commercialization through subsequent R&D development activities.

DLR	Deutsches Zentrum Für Luft - und Raumfahrt e.V.	DE	
FZJ	Forschungszentrum Jülich GmbH	DE	
IREC	Fundacio Institut De Recerca De L'Energia De Catalunya	ES	
HTE	HTE GmbH The High Throughput Experimentation Company	DE	
CSIC	Agencia Estatal Consejo Superior De Investigaciones Científicas	ES	
MAM HW	Morgan Advanced Materials Haldenwanger GmbH	DE	
TITAN	TITAN Cement Company S.A.	GR	
BASF*	BASF SE	DE	

*Associated Partner

Funded by the European Union

Document Summary

The performance of ceramic mixed-ionic electronic conductor (MIEC) membranes, which are critical for high-temperature solar-thermal membrane reactors, is endangered by creep deformation under prolonged mechanical and thermal stress (900–1500 °C). This study systematically evaluates the high-temperature creep behaviour of four potential membrane component materials (gadolinium-doped ceria [GDC-10], zirconia-based solid solutions [8YSZ, CFSZ], and calcium titanate [CTF-10]) under compressive loading, informed by predictive models and prior literature. Experimental campaigns were designed to (1) estimate operational stress limits based on published creep parameters and (2) expand the evaluated stress/temperature range (doubled and tripled from baseline estimates) to identify failure thresholds under air atmosphere (900-1500 °C).

Results reveal clear disparities in mechanical resilience: GDC-10, 8YSZ, and CFSZ exhibited negligible creep below 1200 °C, with deformation remaining undetectable within experimental precision, aligning with their dislocation/microstructural stability under compressive stress. In contrast, CTF-10 demonstrated catastrophic creep and thermal softening at 1200 °C, attributed to iron-doped dislocation mobility, rendering it unsuitable for long-term solar-thermal applications. Among the viable candidates, GDC-10 emerged as the most resilient while 8YSZ/CFSZ showed competitive performance but with slightly higher creep sensitivity at extreme temperatures. The creep rates determined above 1300 °C need to be considered in real operation depending on actual mechanical loads defined by membrane geometry as well as operation conditions. This study provides a quantitative framework for stress/temperature design constraints and highlights GDC-10, 8YSZ and CFSZ as the potentially stable candidates for high-temperature MIEC applications.

Changes with Respect to the DoA

No changes applicable

Funded by
the European Union

Table of Contents

Funded by
the European Union

1. Background: initial considerations

SOMMER project establishes two main initial modes of operation (Figure 1). In both cases, the reactor will consist of a ceramic membrane whose oxygen permeability will be paramount. In the first mode, as shown in Figure 1a, the membrane reactor operates at the high temperatures (1500 °C), achieved using concentrated solar power. Here, in the permeate side, an inert sweep gas (preferably N_2) or a vacuum can be used. With operation conditions at elevated temperatures close to sintering temperatures of the membrane materials under a constant mechanical load, creep is believed to be the most obvious challenge for a reliable mechanical integrity and long-lived performance.

Therefore, the potential membrane materials selected in WT 2.1 for operation in CASE I were creep tested in order to identify creep mechanisms and experimental parameters allowing evaluation of reliability of membrane components made from those materials under real operation conditions. The objective of this report is to first estimate the expected mechanical challenges for the membrane materials. Second with this estimated value samples will be produced and the range will be doubled and tripled to evaluate the creep behaviour within the mechanical load range of interest and temperatures from 900-1500 °C in air giving indications on the creep mechanisms.

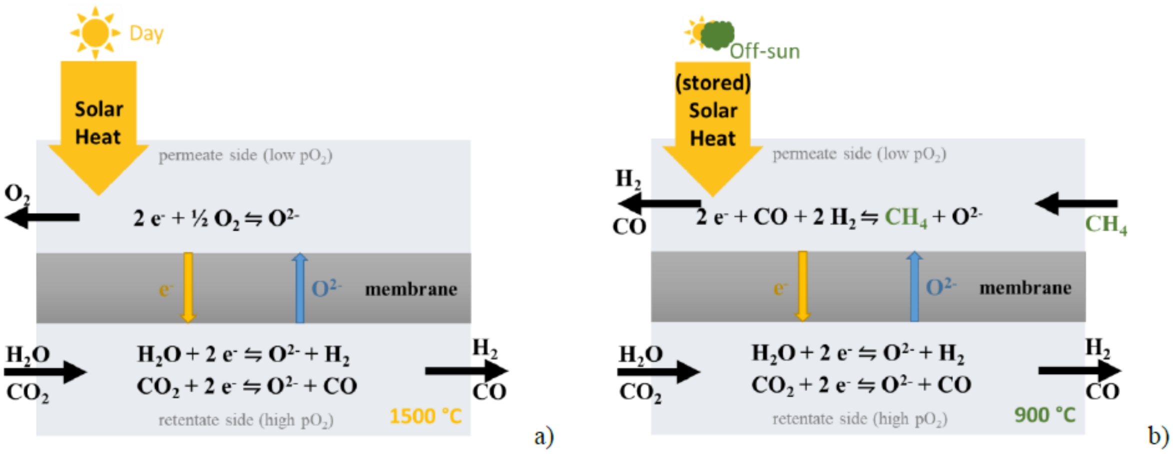

Figure 1. a) High-temperature scenario or CASE I and b) lower temperature scenario or CASEII in which off-sun operation is carried out by supplying a methane (biogas) current on the permeate side, thereby lowering the temperature.

2. Background: creep behaviour of ceramics

Among the leading candidate materials for high-temperature MIEC membranes are gadolinium-doped ceria (GDC-10), zirconia-based solid solutions (e.g., CFSZ, 8YSZ), and calcium titanate (CTF-10), all of which exhibit promising performance in the 900-1500 °C range. Despite their potential, these materials face a critical challenge: creep deformation, a time-dependent, irreversible strain that occurs under constant mechanical load at high temperatures. Even at stresses below the material's yield strength, sustained loading can lead to progressive deformation and eventual mechanical failure which is a

Funded by the European Union

particularly acute concern in membrane reactors, where materials are subjected to combined thermal, mechanical, and chemical stresses over extended durations.

Ceramic membranes, while inherently strong under compression, are brittle under tensile stress. Thus, compressive loading is preferred to maintain structural integrity, while tensile stresses must be minimized through careful reactor design. The steady-state creep rate (denoted as $\dot{\varepsilon}$) is a key parameter for evaluating material resilience and follows a thermally activated power-law relationship:

$$\dot{\varepsilon} = \dot{\varepsilon}_0 \cdot A \cdot (\frac{\sigma}{\sigma_0})^n \cdot e^{-\frac{E_a}{RT}} \quad (1)$$

Here, A is a material constant (Dorn constant), n the stress exponent, E_a the activation energy, R the gas constant, and $\dot{\varepsilon}_0$ and σ_0 are reference values of 1 s^{-1} and 1 MPa, respectively.

Previous studies provide valuable insights into the creep behavior of these materials. For GDC, Lipińska-Chwałek et al. examined porous CeO_2 (1600 °C sintered, 24 % porosity), finding that at 900 °C and 30-120 MPa, the material exhibited a stress exponent (n = 2.3 ± 1.1) and an activation energy (Ea = 160 ± 60 kJ/mol), suggesting dislocation-mediated deformation[1]. In contrast, Routbort et al. studied dense GDC-10 at 1200-1300 °C, reporting a higher (E_a = 480 ± 100 kJ/mol) with (n = 1.3 ± 0.2), indicative of grain-boundary diffusion control [2]. For GDC-20, higher dopant levels improved creep resistance, with E_a values ranging from 60 to 100 kJ/mol at 800-900 °C [1].

In YSZ, Owen and Chokshi proposed that polycrystalline 3YSZ exhibits two distinct creep regimes: a high-stress dislocation mechanism (n ≈ 2) and a low-stress diffusion-controlled process (n ≈ 3), both with (E_a ≈ 550 kJ/mol) [3]. Later, Berbon and Langdon suggested an alternative interface-controlled diffusion creep model [4]. For 6YSZ, Jiménez-Melendo et al. observed tetragonal-phase creep at 1250–1450 °C, with (n = 1.4) and (E_a = 491 kJ/mol), while single-crystal YSZ demonstrated dislocation-dominated creep (n ≈ 4) at 1650-1850 °C, with (E_a = 400-500 kJ/mol) [5].

For calcium titanate (CTF-10), Li et al. reported high activation energies (E_a ≈ 750 kJ/mol) at 1180-1218 °C), dropping to 500 kJ/mol at 1250-1300 °C, along with a low-stress creep exponent (n = 1), suggestive of grain-boundary diffusion (Coble creep). [6]

Nonetheless, creep behaviour at temperatures up to 1500 °C as considered in solar-thermal applications for poly-crystallin materials are not yet reported.

3. Stress estimation at operation conditions

As a starting point, the expected stresses need to be estimated. According to the introduced operation conditions using argon or vacuum on the sweep side to ensure an oxygen partial pressure gradient the vacuum is believed to be more challenging as it introduces a pressure gradient across the membrane, i.e. ~ 1 bar. For the operation conditions a tubular design is beneficial. Given the enhanced compressive stress resistance of ceramics over tensile stresses the membrane reactor should be operated with a lower pressure on the inside compared to the outside of the tube reactor.

Using this membrane geometry and the pressure difference, initial stress considerations are made. Formulas (2) to (6) below can be used to estimate the stresses occurring in tubes subjected to external pressure.

Funded by
the European Union

(2) Tangential stress (σ_t) with external pressure:

$$\boldsymbol{\sigma_t = -p_e * \frac{r_e^2}{r_e^2 - r_i^2} * (1 + \frac{r_i^2}{r_x^2})}$$

(3) Radial stress (σ_r) with external pressure:

$$\sigma_r = -p_e * \frac{r_e^2}{r_e^2 - r_i^2} * (1 - \frac{r_i^2}{r_x^2})$$

(4) Longitudinal stress (σ_l) with external pressure:

$$\sigma_l = \frac{(p_i * r_i^2 - p_e * r_e^2)}{(r_e^2 - r_i^2)}$$

(5) Maximum for r_x=r_i

$$\boldsymbol{\sigma_t = -p_e * \frac{r_e^2}{r_e^2 - r_i^2} * 2}$$

(6) Maximum for r_x=r_e

$$\sigma_r = -p_e * \frac{r_e^2}{r_e^2 - r_i^2} * (1 - \frac{r_i^2}{r_e^2})$$

It is evident that the maximum value for equation (5) will always be twice the value of equation (6). Therefore, the tangential stress with the maximum observed values is used for operational stress estimation.

Consequently, tangential stresses for tubes within a broader range of possible geometries are calculated, with wall thicknesses ranging from 0.1 to 1 mm and outside diameters from 1 to 20 mm. The results, visualized in Figure 2, demonstrate the expected parabolic increase of pressure tangential stresses (σ_t) with smaller wall thicknesses.

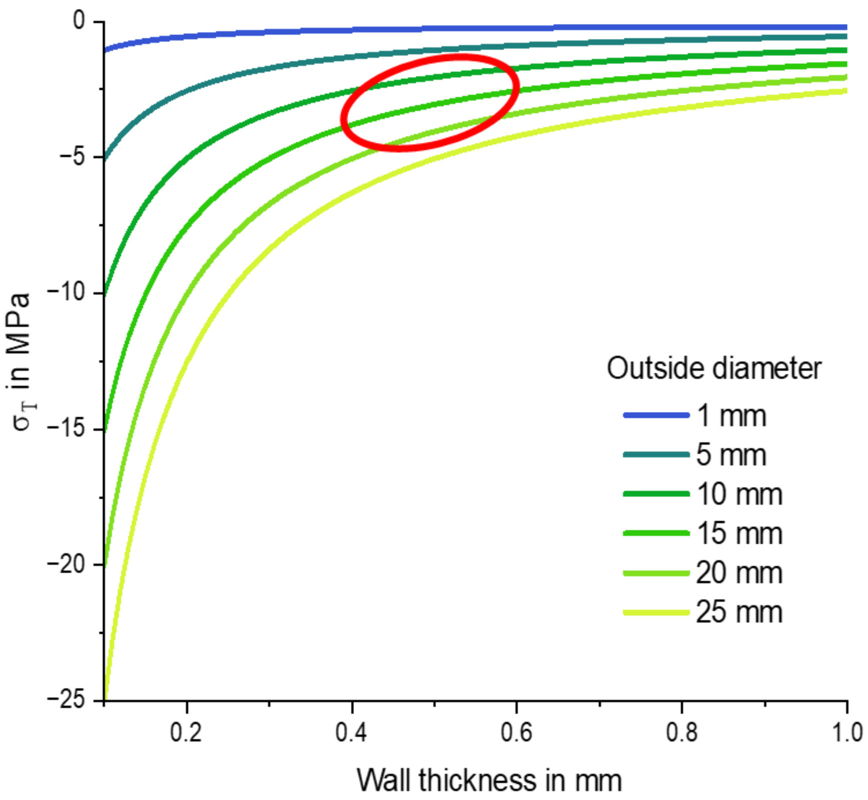

Figure 2: Estimated tangential stresses for tubular membrane reactors within a feasible range of outside diameters of 1 to 25 mm and wall thickness of 0.1 to 1.0 mm

To estimate realistic pressure stresses, only theoretically manufacturable tube geometries are considered. Therefore, only stresses of tubes with outer diameters of 10 to 20 mm and wall thicknesses of 0.4 to 0.6 mm are highlighted in the red oval. Within this range, compressive tangential stress of about 5 MPa can be expected. To make sure to get into a measurable range this stress is also extended to the twofold and threefold to a compressive stress range of 5, 10, and 15 MPa for creep testing at

Funded by
the European Union

up to 1500 °C in air for the selected materials using sample bars with 5x5 cm^2 cross section under constant compressive loads.

4. Creep analysis of the selected membrane materials

The experimental investigation into the creep behaviour of the selected ceramic materials has revealed a pronounced hierarchy in their resistance to time-dependent deformation under compressive loading. A conventional benchmark commonly is that a creep strain below 1% per year is considered non-critical and it is notable that such low strains remain undetected within the resolution limits of the current experimental setup. The analysis of the Arrhenius plot (Figure 3), which maps the steady-state creep rate against the reciprocal of absolute temperature (900-1500 °C) under compressive stresses of 5, 10, and 15 MPa, provides insights into the temperature-dependent deformation mechanisms governing each material. CTF-10 exhibits measurable creep rates even at 900 °C already under applied stress of 5 MPa. In contrast, CFSZ and 8YSZ only begin to demonstrate detectable deformation above 1200 °C, while GDC-10 maintains non-detectable strain until approximately 1300 °C. Beyond 1000 °C, CTF-10 undergoes a dramatic loss of mechanical cohesion, adopting a behaviour characteristic of viscous fluids. This deviation underscores its inferior performance in high-temperature applications.

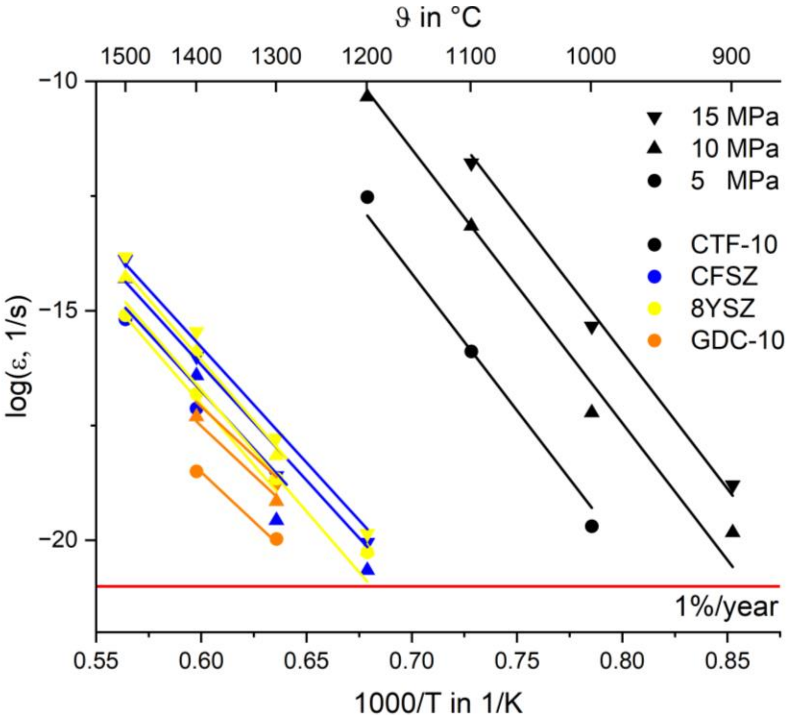

Figure 1: Arrhenius plot from 900-1500 °C in air with compressive stresses between 5-15 MPa

The slopes of these plots facilitate the determination of the activation energy (E_a), a parameter that quantifies the energy barrier for thermally activated creep processes listed in Table 1. Complementing this, the double-logarithmic stress-creep relationship at constant temperatures (Figure 4) reveals how the creep rate scales with applied stress, with the derived stress exponent (n) elucidating the mechanistic sensitivity to stress.

Funded by the European Union

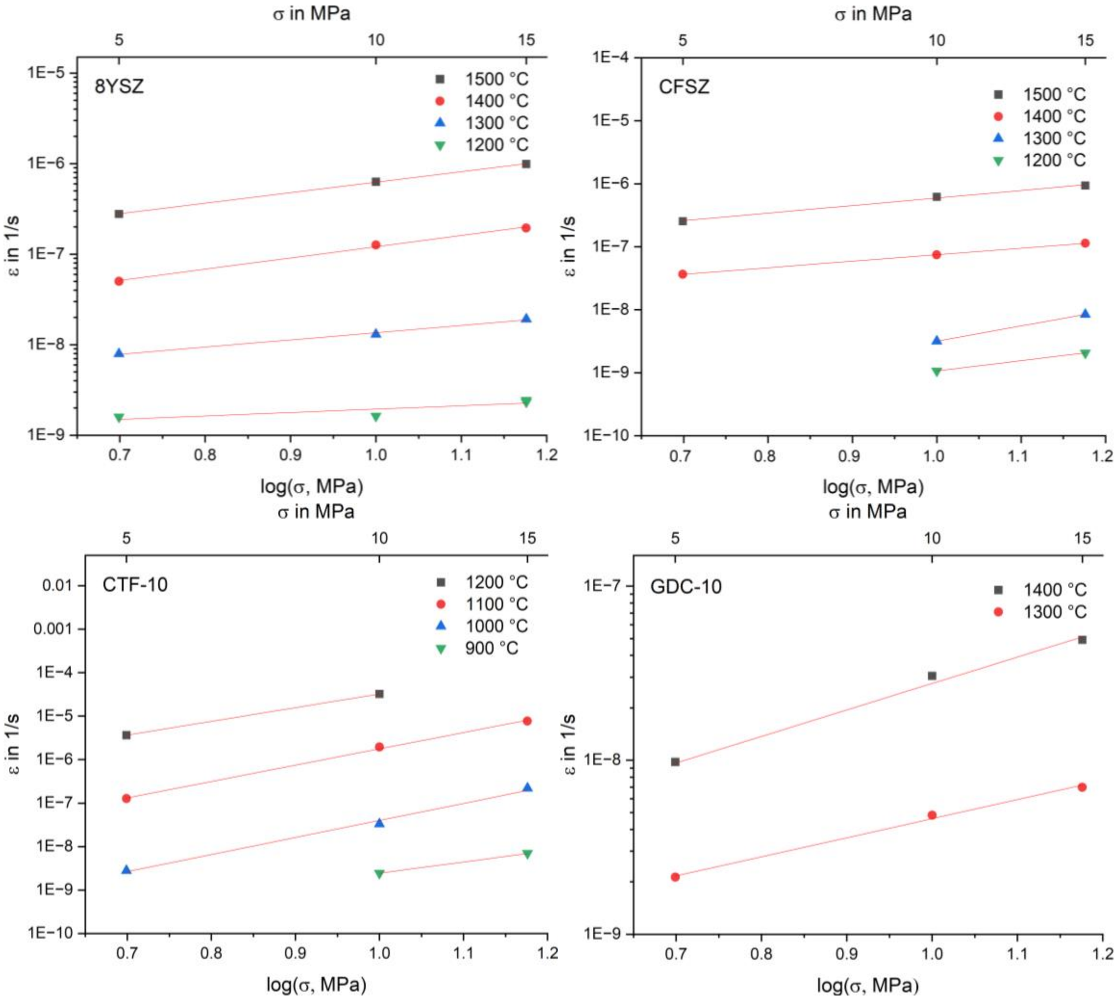

Figure 2: Double-logarithmic plots of the creep rates as a function of applied compressive stresses at shown temperatures

By applying the steady-state creep rate formula (1), the relevant parameters could be systematically extracted in table 1 for direct comparison. The results indicate that CTF-10 possesses an activation energy of 440 ± 40 kJ/mol and a stress exponent of 3.0 ± 1.0, values that contrast sharply with the diffusional-dominated behaviour observed in 8YSZ, CFSZ, and GDC-10. Notably, GDC-10 presents a broader range of activation energies (241-426 kJ/mol), introducing variability that complicates a unified mechanistic interpretation.

Table 1: Stress exponents for materials

Material	Activation energy in kJ/mol	Stress exponent	ϑ range in °C
GDC-10	$3{\cdot}10^2 \pm 1{\cdot}10^2$	1.3 ± 0.3	1400-1300
8YSZ	$4.2{\cdot}10^2 \pm 0.4{\cdot}10^2$	0.9 ± 0.4	1500-1200
CFSZ	$5{\cdot}10^2 \pm 0.5{\cdot}10^2$	1.5 ± 0.6	1500-1200
CTF-10	$4.4{\cdot}10^2 \pm 0.4{\cdot}10^2$	3 ± 1	1200-900

The dominant creep mechanisms can be estimated by these values. CTF-10, with its elevated stress exponent ($n \approx 3$) and moderate activation energy, seems to align with dislocation-controlled creep,

Funded by the European Union

wherein thermally activated dislocation climbs dictate deformation kinetics. This behaviour diverges markedly from the diffusional creep regime exhibited by 8YSZ and CFSZ, both of which demonstrate stress exponents near unity with a hallmark of grain boundary sliding or lattice diffusion. The case of CFSZ, with a stress exponent of 1.5 ± 0.6, suggests a transitional state between these mechanisms, possibly influenced by grain size distributions or effects of monoclinic precipitates found after annealing tests at high temperatures. For GDC-10, the observed variability in activation energy, coupled with a stress exponent of 1.3 ± 0.3, reinforces its alignment with diffusional creep, albeit with greater sensitivity to microstructural fluctuations than the other materials.

When contextualized within existing literature, these findings yield additional perspective. CTF-10, despite its compositional similarity to pure $CaTiO_3$, exhibits accelerated degradation above 1200 °C, a deviation attributed to the destabilizing influence of iron doping. While the activation energy for CTF-10 (≈500 kJ/mol) remains consistent with values reported by Li et al. for temperatures between 1250-1300 °C, the substantially higher stress exponent ($n \approx 3$) signifies a shift toward dislocation-mediated deformation, likely due to the introduction of iron impurities [6]. Meanwhile, the activation energies and stress exponents for 8YSZ and CFSZ exhibit strong concordance with those of tetragonal 6YSZ, affirming their mechanical resilience under high-temperature conditions[4]. GDC-10, although demonstrating agreement with Routbort's observations, deviates from the findings of Lipinska et al., a discrepancy that may stem from differences in grain boundary chemistry or sintering treatments [1,2].

5. Conclusions

The present study has systematically evaluated the high-temperature creep behaviour of four ceramic materials under compressive loading, revealing critical distinctions in their suitability for applications demanding prolonged structural integrity. GDC 10, 8YSZ and CFSZ exhibited exceptionally low creep rates at temperatures below 1200 °C, with no measurable deformation detected within the resolution limits of the experimental setup, a performance consistent with their classification as highly creep-resistant candidates for advanced structural applications. In contrast, CTF 10 demonstrated a catastrophic loss of mechanical stability at 1200 °C, characterized by thermal softening and irreversible deformation, thereby precluding its applicability in scenarios where long-term dimensional fidelity is required. This failure mode, directly attributable to iron doping-induced dislocation mobility, underscores its fundamental instability under conditions relevant to solar-thermal applications, where thermal and mechanical demands are stringent.

While 8YSZ, CFSZ, and GDC 10 collectively exhibit modest yet manageable creep rates under the tested conditions, their performance remains highly competitive for high-temperature service, particularly when operational temperatures are confined below 1300 °C. GDC 10, in particular, demonstrates superior resilience, maintaining structural coherence even as it approaches the upper limits of the evaluated temperature range. Nevertheless, these findings must be contextualized within broader environmental considerations, as real-world deployment often involves exposure to reactive atmospheres, such as those containing CO_2, H_2O, or fluctuating oxygen partial pressures, which may introduce corrosive or oxidation-mediated degradation mechanisms not captured in the present air-based experiments.

Funded by the European Union

6. Bibliography

[1] Lipińska-Chwałek M, Pećanac G, Malzbender J. Creep behaviour of membrane and substrate materials for oxygen separation units. Journal of the European Ceramic Society 2013;33:1841–8. https://doi.org/10.1016/j.jeurceramsoc.2013.02.007.

[2] de Arellano-L AR, Wolfenstine J. J.L. Routbort and K.C. Goretta n.d.

[3] Owen DM, Chokshi AH. The high temperature mechanical characteristics of superplastic 3 mol% yttria stabilized zirconia. Acta Materialia 1998;46:667–79. https://doi.org/10.1016/S1359-6454(97)00251-6.

[4] Berbon MZ, Langdon TG. An examination of the flow process in superplastic yttria-stabilized tetragonal zirconia. Acta Materialia 1999;47:2485–95. https://doi.org/10.1016/S1359-6454(99)00099-3.

[5] Jiménez-Melendo M, Domínguez-Rodríguez A. High temperature mechanical characteristics of superplastic yttria-stabilized zirconia. An examination of the flow process. Acta Materialia 2000;48:3201–10. https://doi.org/10.1016/S1359-6454(00)00113-0.

[6] Li P, Karato S, Wang Z. High-temperature creep in fine-grained polycrystalline $CaTiO_3$, an analogue material of (Mg, Fe)SiO_3 perovskite. Physics of the Earth and Planetary Interiors 1996;95:19–36. https://doi.org/10.1016/0031-9201(95)03107-3.

[7] Li X, Gonzalez-Julian J, Malzbender J. Fabrication and mechanical performance of Ti_2AlN prepared by FAST/SPS. Journal of the European Ceramic Society 2020;40:4445–53. https://doi.org/10.1016/j.jeurceramsoc.2020.05.017.

[8] Deibert W, Stournari V, Ivanova ME, Escolástico S, Serra JM, Malzbender J, et al. Effect of microstructure on electrical and mechanical properties of $La_{5.4}WO_{12-\delta}$ proton conductor. Journal of the European Ceramic Society 2018;38:3527–38. https://doi.org/10.1016/j.jeurceramsoc.2018.04.009.

[9] Rutkowski B, Malzbender J, Beck T, Steinbrech RW, Singheiser L. Creep behaviour of tubular $Ba_{0.5}Sr_{0.5}Co_{0.8}Fe_{0.2}O_{3-\delta}$ gas separation membranes. Journal of the European Ceramic Society 2011;31:493–9. https://doi.org/10.1016/j.jeurceramsoc.2010.10.030.

Funded by the European Union